Desalination and Water Treatment
www.deswater.com
1944-3994/1944-3986 © 2013 Desalination Publications. All rights reserved
doi: 10.1080/19443994.2012.693658

51 (2013) 1443–1456
February

Taylor & Francis
Taylor & Francis Group

Uncertainty analysis of COP prediction in a water purification system integrated into a heat transformer using several artificial neural networks

J.A. Hernández[a], D. Colorado[b,*]

[a]*Centro de Investigación en Ingeniería y Ciencias Aplicadas (CIICAp), Universidad Autónoma del Estado de Morelos (UAEM), Av. Universidad 1001. Col. Chamilpa, C.P. 62209, Cuernavaca, Morelos, México*
[b]*Centro de Investigación en Recursos Energéticos y Sustentables (CIRES), Universidad Veracruzana, Av. Universidad km 7.5, Col. Santa Isabel, C.P. 96535, Coatzacoalcos, Veracruz, Mexico*
Tel. +921 203 65 16; emails: dcolorado@uv.mx; dario_colorado@uaem.mx

Received 20 February 2012; Accepted 10 May 2012

ABSTRACT

Numerous authors have reported the prediction of performance of heat pumps using artificial neural networks. However, the accuracy of the calculation is generally unknown. Four feedforward networks with one hidden layer are developed and used in order to obtain coefficient of performance (COP) prediction. COP permitted us to evaluate a water purification process integrated into a heat transformer. For the networks, the logarithmic sigmoid (LOGSIG), the hyperbolic tangent sigmoid (TANSIG) and the linear (PURELIN) transfer function were used. In the validation process, effects over regression coefficient, slope and intercepts with different input normalization ranges were evaluated. Input normalization range from −1 to 1 with TANSIG in hidden layer and without uncertainty in the input variables presented better results in comparison with other normalization ranges. However, Monte Carlo method was also applied in order to obtain error propagation COP prediction (using relative standard deviation, $\%RSD_{COP}$), with the aim to determine confidence level of models. Effects over $\%RSD_{COP}$ with different input normalization ranges were evaluated for the development of four neural network models. Input normalization range from 0 to 1 with TANSIG in hidden layer and with uncertainty in the input variables presented better results in comparison with other normalization ranges.

Keywords: Error propagation; Monte Carlo method; Logarithmic sigmoid; Hyperbolic tangential

1. Introduction

Artificial neural networks (ANNs) have been used in diverse applications such as robotics, pattern recognition forecasting, medicine, power systems, manufacturing, signal processing, social/psychological science, online state estimation and control of drying processes, business, electronics, entertainment, oil and gas

*Corresponding author.

Presented at the International Conference on Desalination for the Environment, Clean Water and Energy, European Desalination Society, 23–26 April 2012, Barcelona, Spain

production, transportation, geothermometry, seawater desalination system, processes to obtain drinking water, and equation fitting in critical values. This approach has also been used for the determination of thermodynamic properties (LiBr–water and LiCl–water solutions) and applications in energy processes for their optimization [1–7].

Today, obtaining pure water is a serious problem all over our planet. In this work, the water purification system used was a distillation process in which impure water is heated to obtain vapor that is immediately condensed, yielding heat and pure water [8]. The absorption heat transformer is a system that consists of a thermodynamic device capable of producing useful heat at a thermal level superior to the one at the source [9]. According to a number of published papers, for example Holland et al. [8] and Santoyo-Gutiérrez et al. [9], it is possible to combine the heat transformer with a water purification process. This combination enables us to increase the temperature of the impure water system, and thus, purer water is obtained.

There are four main components in the energy cycle of an absorption heat transformer (Fig. 1): the absorber (AB), the evaporator (EV), the generator (or desorber) (GE) and the condenser (CO). Quality of waste heat Q_{GE} is added at a relatively low temperature to the generator to vaporize the water from the weak salt solution containing a low concentration of lithium bromide. The vaporized water flows to the condenser, delivering an amount of heat Q_{CO} at a reduced temperature T_{CO}. According to Rivera [10],

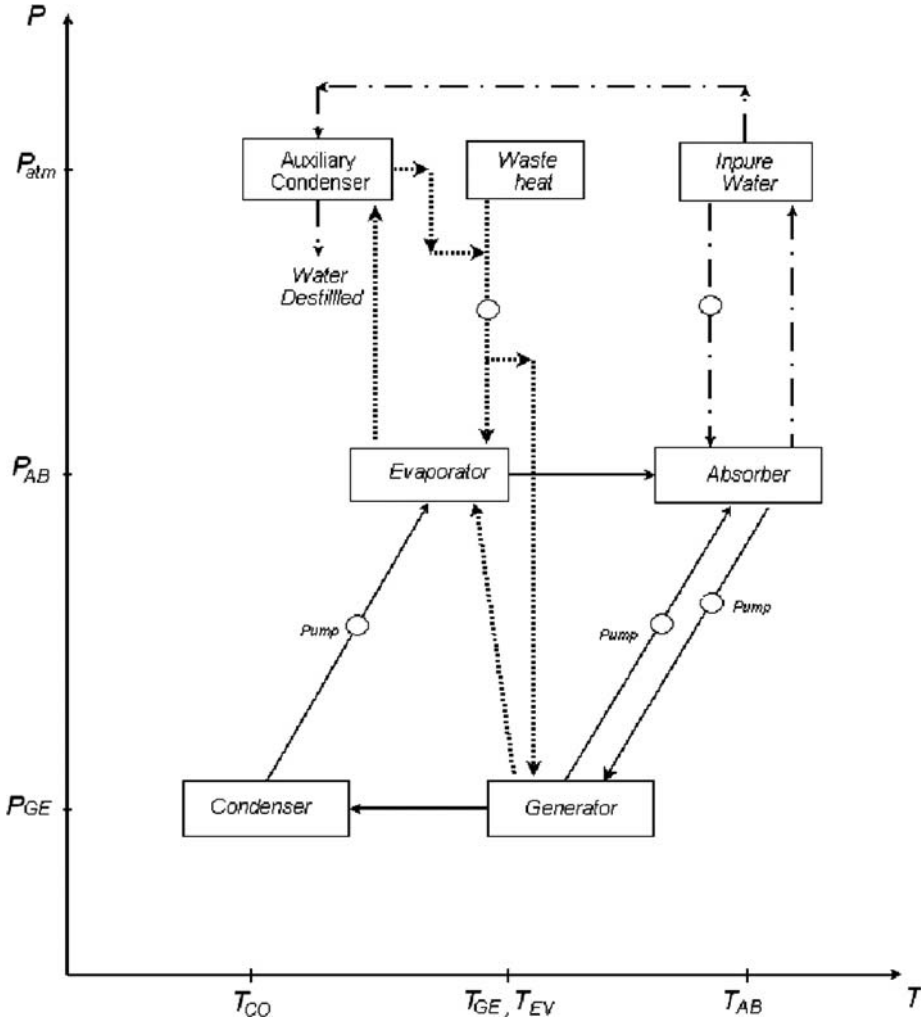

Fig. 1. Schematic diagram of the integration of the water purification process to an absorption heat transformer with energy recycling. The continuous line (-) represents the absorption heat transformer, the dash dot (-··-) represents the water purification process and the dotted lines (…) are the recycling energy.

the liquid water leaving the condenser is pumped to the evaporator, where it is evaporated using quantity of waste heat Q_{EV} at an intermediary temperature T_{EV}. Next, the vaporized water flows to the absorber, where it is absorbed in a strong salt solution coming from the generator, and delivers heat Q_{AB} at a high temperature T_{AB}. Finally, the weak salt solution is returned to the generator and the cycle is repeated. In this type of energy cycle (absorption heat transformer), the coefficient of performance (COP) is a very important parameter that defines the efficiency of the heat transformer [8].

The COP is defined (Eq. (1)) by the ratio of heat delivered in the absorber (Q_{AB}) to the heat load supplied to the generator (Q_{GE}) and the evaporator (Q_{EV}).

$$\mathrm{COP} = \frac{Q_{AB}}{Q_{GE} + Q_{EV}} \tag{1}$$

Siqueiros and Romero [11] proposed a water purification system using an absorption heat transformer, in which part of the total heat upgraded by the heat transformer is recycled. In this system, the COP values are improved by energy recycling because part of the heat is used to increase the heat source temperature. Siqueiros and Romero [11] reported $\mathrm{COP_{WP}}$ for water purification (WP) process with energy recycling as follows:

$$\mathrm{COP_{WP}} = \frac{\mathrm{COP}}{1 - \eta \mathrm{COP}} \tag{2}$$

where

$$\eta = \frac{\Delta H_v}{H_v + H_s} \tag{3}$$

The term η is the ratio of latent heat to the summation of latent and sensible heat from the absorber.

Several thermodynamic models have been reported for heat transformers. Huicochea and Siqueiros [12] presented theoretical results obtained with a thermodynamic model to describe a water purification process integrated into heat transformer using different configurations while energy is recycled. Also, Siqueiros and Romero [11] reported the increase in COP for an absorption heat transformer. These models involved analytical solution and global balances according to the physic and thermodynamic of an absorption system. Likewise, in order to simplify this complex system, ANNs have been used to describe absorption systems. ANN models are recommended by several authors to estimate the performance of energy and thermal systems. Hernández et al. [5,13] developed a forecasting model for a water purification process integrated into an absorption heat transformer, using ANN for the online prediction of COP. Hyperbolic tangential (TANSIG) transfer function in the hidden layer has been used. Also, Sozen et al. [14] proposed an ANN technique as an approach to determine the exergy losses of an ejector absorption heat transformer. Logarithmic sigmoid (LOGSIG) transfer function has been used, and comparison between conjugate gradient and Levenberg–Marquardt optimization methods was made by the authors. Mohanraj et al. [15] used the ANN to simulate a performance prediction of a direct-expansion solar-assisted heat pump. Two neurons in the input layer represent that a solar intensity and ambient temperature were used in order to predict power consumption, heating capacity, energy performance ratio and compressor discharge temperature, while ten neurons were used in the hidden layer with logistic sigmoid transfer function. Others methods to predict performance of energy system are being developed and these are compared with ANN results. Esen et al. [16] compared an ANN to statistical weighted pre-processing (SWP) method with ANN applied to predict the performance of a horizontal ground source heat pump with R-22 for a heating configuration. In the same flame of heat pumps, Esen and Inalli [17] described the availability of an Adaptive Neuro-Fuzzy Inference System (ANFIS) and ANN models on vertical ground source heat pump for cooling and heating configurations; ANFIS is highlighted as more efficient in forecasting performance that ANN using the minimum data set. Studies of appropriate normalization range in the input layer and confidence intervals of ANN models are not presented in the literature. In many cases, validation of the physical models (empirical or theoretical) is based on the simple comparison of the prediction with the experimental results, without taking into account the respective uncertainties. To remedy this situation, appropriate confidence intervals of COP for a heat transformer in water purification systems should be experimentally determined.

Traditionally, error propagation is determined using equations proposed by Bevington and Robinson [18]. Error propagation from Monte Carlo method represents an alternative that consists of a repeated calculation of a quantity, varying each time the input data randomly within their stated prediction limits [19]. Anderson [19] described the Monte Carlo method as inefficient due to its long calculation time, but today due to the availability of fast computers, application of this procedure is not a difficult task.

According to Rees [20], the standard deviation, σ, of a function of type:

$$y = f(x_1, x_2 \ldots, x_n) \quad (4)$$

is given by

$$\sigma_y^2 = \sum_{i=1}^{n} \left(\frac{\partial y}{\partial x_i}\right)^2 \sigma_{Xi}^2 \quad (5)$$

where σ_{Xi} is the standard deviation of X_i and the variable x_i is independent.

Recently, Colorado et al. [21] demonstrated a way to determine the error propagation of COP into an absorption heat transformer for water purification, using an ANN model. A correlation for $\%RSD_{COP}$ prediction was developed based on introduced errors in the input operation variables, however valid only for the ANN architecture and a transfer function investigated during the numerical studies.

Consequently, the objective of the present work is to develop four ANN models without errors in the input variables and evaluate the influence of input normalization ranges and transfer functions in the hidden layer to predict COP in the validation process using statistical tools. Then, in this work, different levels of errors were considered in the input variables, with the aim to obtain standard deviation of COP values and to find the most accurate transfer function using the error propagation analysis. These equations were obtained through ANN from experimental data of the integration of a water purification process into an absorption heat transformer with energy recycling. An input variable ANN was recaptured by Hernández et al. [13] for COP prediction.

2. Experimental data

Fig. 1 shows a schematic diagram of the absorption heat transformer integrated into a water purification process. The absorber gives a useful heat quantity Q_{AB}, produced by the heat transformer from the evaporator, condenser and generator [11].

Experimental database consists of different COP values, obtained from a portable water purification process coupled to an absorption heat transformer with energy recycling. The experimental data set was obtained at different initial concentrations of $LiBr-H_2O$, different temperatures in the absorber, the generator, the evaporator and the condenser, and different pressures in the absorber and the generator. In addition to the experimental data of each component, the transitory and steady state were taken into account for each initial concentration applied in the process. Data were collected during 4 and 2 h after start-up. These parameter changes and data acquisition allowed us to obtain experimental information that was sufficient to develop the neural network

Table 1
Experimental operation range conditions studies to obtain the COP values

Input	Temperature (°C)	Limiting conditions studies	Instrumentation label (see Fig. 4)
1	$T_{inGE\text{-}AB}$	76.29–91.53	T1
2	$T_{inEV\text{-}AB}$	74.56–89.93	T2
3	$T_{outAB\text{-}GE}$	84.31–98.27	T3
4	$T_{inAB\text{-}GE}$	74.99–92.58	T4
5	$T_{outGE\text{-}CO}$	76.29–91.53	T5
6	$T_{outGE\text{-}AB}$	77.03–83.89	T6
7	T_{inCO}	40.37–65.03	T7
8	T_{outCO}	26.77–33.79	T8
9	T_{inEV}	28.52–85.33	T9
10	$T_{outEV\text{-}AB}$	74.56–89.93	T10
	Concentration%		
11	XinAB	51.66–55.36	X1
12	XoutAB	50.75–54.36	X2
13	XinGE	50.75–54.36	X3
14	XoutGE	53.16–56.07	X4
	Pressure in Hg, (absolute)		
15	PAB	7.00–11.50	P1
16	PGE	19.00–21.10	P2

Table 2
Some experimental data studies to obtain the COP values

k	Input	A	B	C	D	E	F	G
1	$T_{\text{in.GE-AB}}$	79.89	86.32	86.47	86.26	89.27	87.73	89.64
2	$T_{\text{in.EV-AB}}$	85.61	81.08	80.10	80.31	81.02	81.76	79.61
3	$T_{\text{out AB-GE}}$	91.52	96.79	95.82	94.67	96.31	94.08	95.10
4	$T_{\text{in.AB-GE}}$	88.00	88.43	88.36	88.31	87.85	87.95	89.12
5	$T_{\text{out GE-CO}}$	79.89	86.32	86.47	86.26	89.27	87.73	89.64
6	$T_{\text{out GE-AB}}$	81.78	81.69	81.85	81.82	81.65	81.25	82.51
7	$T_{\text{in.CO}}$	42.67	58.97	58.43	58.10	56.68	56.20	42.32
8	$T_{\text{out.CO}}$	30.45	32.54	32.74	32.93	33.14	33.24	28.52
9	$T_{\text{in.EV}}$	33.22	33.98	34.30	34.14	33.88	34.67	36.50
10	$T_{\text{out.EV-AB}}$	85.61	81.08	80.10	80.31	81.02	81.76	79.61
11	$X_{\text{in.AB}}$	55.25	55.25	55.25	55.25	55.25	55.25	55.31
12	$X_{\text{out.AB}}$	54.33	54.33	54.33	54.33	54.33	54.33	54.33
13	$X_{\text{in.GE}}$	54.33	54.33	54.33	54.33	54.33	54.33	54.33
14	$X_{\text{out.GE}}$	55.97	55.97	55.97	55.97	55.97	55.97	56.07
15	P_{AB}	9.00	9.00	9.00	9.00	9.00	9.00	11.00
16	P_{GE}	21.10	21.10	21.10	21.10	21.10	21.10	21.00
	COP_{EXP}	0.21	0.24	0.27	0.30	0.33	0.36	0.39

model [13]. A summary of the limiting-conditions studies for the operation parameters used in the experimental database is presented in Table 1.

The thermodynamic properties of the LiBr−H_2O mixture were estimated with Alefeld correlations cited by Torres-Merino [23]. The input and output temperatures of each component (AB, GE, CO and EV) were obtained experimentally. At the same time the pressure of two components (AB and GE) was registered with a temperature-pressure acquisition system (thermocouple conditioner and Agilent equipment with commercial software). The input and output concentrations in the AB and GE were established by a refractometer (refraction index). In this process, LiBr + H_2O was used as the working fluid in the absorber and generator, while only H_2O was used in the evaporator and condenser.

Table 2 shows experimental information in a COP range from 0.21 to 0.39. As many as 16 variables are used and registered: 10 temperatures, 4 concentrations and 2 levels of pressure.

3. Artificial neural modeling

ANN was used to predict COP in a water purification system integrated into a heat transformer with energy recycling. Four models are developed using hyperbolic tangent sigmoid and logarithmic sigmoid transfer function in hidden layer, considering linear transfer function in output layer. Development of these models was carried out without considering the uncertainty in the input variables. Different normalization ranges in the input variables were used to evaluate the effect over ANN prediction. Experimental database is split into 50% for learning and 50% for testing to get a good representation of the diversity of the operating conditions. The coefficients of the network (weight W and bias B) and the number of iterations of the optimization algorithm are calculated during the training stage, thus minimizing a root mean square error (RMSE) between simulated and experimental data. In this work, for the learning process, we fixed the number of neurons in the hidden layer as two. The optimum model is that which introduces minimal error. In this research, Levenberg–Marquardt method algorithm of optimization was used. In the following section, four ANNs are developed and described.

3.1. Logarithmic sigmoid function and input normalization range between 0 and 1

A neural network with two neurons in the hidden layer was found to be efficient in predicting the COP. For this model, logarithmic sigmoid transfer function in hidden layer and linear transfer function in output layer were applied. Fig. 2(a) presents a comparison between experimental and simulated COP values using the learning and test database. The input normalization range was 0 to 1 given by

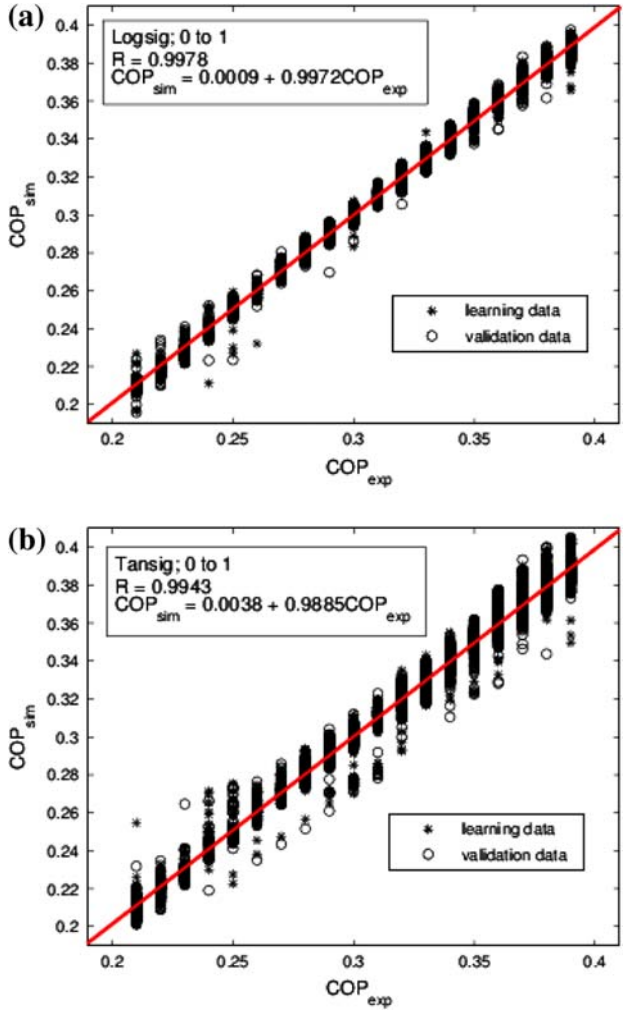

Fig. 2. (a) Experimental vs. simulated COP for all the learning and test database using LOGSIG function in hidden layer. (b) Experimental vs. simulated COP for all the learning and test database using TANSIG function in hidden layer.

$$\phi_n = \frac{\phi}{1.01 \cdot \max(\phi)} \tag{6}$$

where ϕ is the input variable (temperature, pressure and concentration) and ϕ_n is the normalized variable.

Comparison between experimental and simulated COP values is made. As a result of this comparison, the value of regression coefficient of learning and testing database was of $R = 0.9978$.

The proposed model using logarithmic sigmoid transfer function in hidden layer and linear transfer function in output layer shown in Fig. 2(a) is represented by the following equation:

$$\mathrm{COP} = \sum_{s=1}^{S} [Wo(1,j) \cdot \left(\frac{1}{1 + \exp(-1 \cdot (\sum_{k=1}^{K} ((W_i(j,k) \cdot \phi_n(k)) + b1(j))))} \right)] + b2 \tag{7}$$

where s is the number of neurons in the hidden layer ($S = 2$), k is the number of neurons in the input layer ($K = 16$) and W and b are weights and biases, respectively.

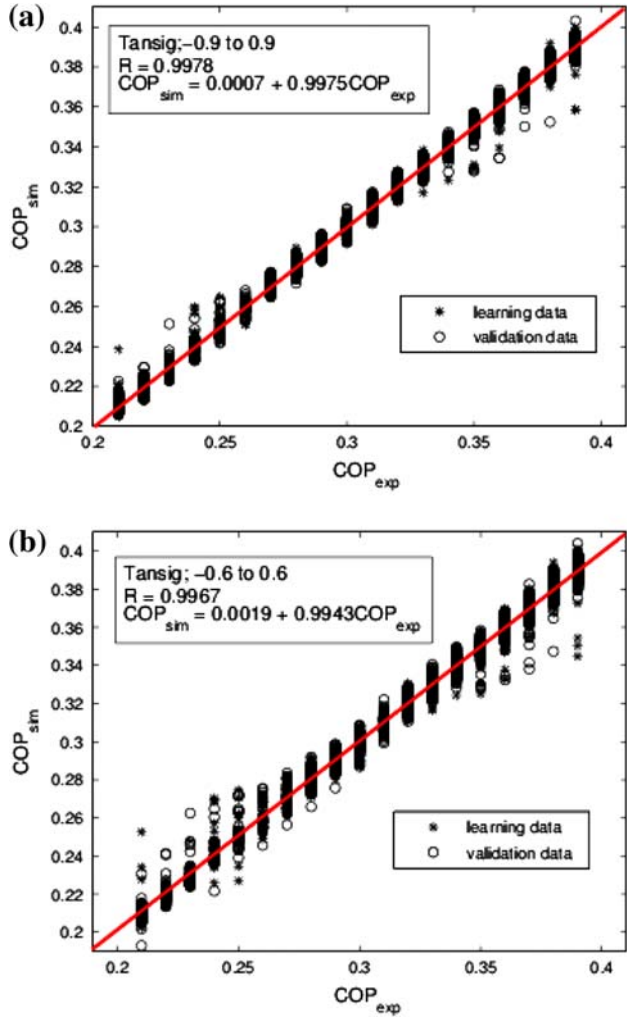

Fig. 3. (a) Experimental vs. simulated COP for all the learning and test database using TANSIG transfer-function in hidden layer and input layer normalization from −0.9 to 0.9. (b) Experimental vs. simulated COP for all the learning and test database using TANSIG transfer-function in hidden layer and input layer normalization from −0.6 to 0.6.

3.2. Hyperbolic tangent sigmoid and input normalization range between 0 and 1

Fig. 2(b) presents a comparison between experimental and simulated COP values using the learning and testing database. For this model, hyperbolic tangent sigmoid transfer function in hidden layer and linear transfer function in output layer were applied. The input normalization range is 0 to 1 as given by Eq. (6).

Comparison between experimental and simulated data of COP values was made. The obtained value of the regression coefficient for learning and testing database is $R = 0.9943$.

This second model is represented in Fig. 2(b), which is described by the following equation:

$$\mathrm{COP} = \sum_{s=1}^{S} Wo(1,j) \cdot \left(\frac{2}{1 + \exp(-2 \cdot (\sum_{k=1}^{K} ((W_i(j,k) \cdot \phi_n(k)) + b1(j))))} - 1 \right) + b2 \tag{8}$$

where s is the number of neurons in the hidden layer ($S = 2$), k is the number of neurons in the input layer ($K = 16$), and W and b are weights and biases, respectively.

3.3. Hyperbolic tangent sigmoid and input normalization range between −0.9 and 0.9

Here different ranges of normalization in ANN are used. For this model hyperbolic tangent sigmoid transfer function in hidden layer and linear transfer function in output layer were applied. Fig. 3(a) presents a comparison between experimental and simulated COP values using the learning and testing database. The input normalization range is −0.9 to 0.9, as given by

$$\phi_n = 0.9 \left[\frac{2\phi - \max(\phi) - \min(\phi)}{\max(\phi) - \min(\phi)} \right] \tag{9}$$

Comparison between experimental and simulated COP values is made, and the value of regression coefficient of learning and testing database of $R = 0.9967$ is obtained.

3.4. Hyperbolic tangent sigmoid and input normalization range between −0.6 and 0.6

Fig. 3(b) presents a comparison between experimental and simulated COP values using the learning and testing database. For this model, hyperbolic tangent sigmoid transfer function in hidden layer and linear transfer- function in output layer were applied. The input normalization range is −0.6 to 0.6, as given by:

$$\phi_n = 0.6 \left[\frac{2\phi - \max(\phi) - \min(\phi)}{\max(\phi) - \min(\phi)} \right] \tag{10}$$

Comparison between experimental and simulated COP values is made out, and the regression coefficient of learning and testing is $R = 0.9966$.

3.5. Statistical test to confirm accuracy of four ANN models

The statistical test of slope = 1 and intercept = 0 is also carried out to confirm accuracy in all ANN models developed [24]. The four ANN models have confirmed the statistical test.

Tables 3 and 4 list the obtained parameters (*Wi*, *Wo*, *b*1 and *b*2) to the four proposed models with two neurons in the hidden layer in all ANN models. These parameters are used in each proposed model to COP prediction.

4. Error propagation determination

Error propagation calculation using Monte Carlo method is a suitable alternative when the complexity of the model is significant. The method (see Fig. 4) is based on repeated calculations of COP prediction, changing input data every time (16 input variables related to the temperature, pressure and concentration, Fig. 4) by a random selection from its error probability distribution.

Different instrumentations were used in the heat transformer, according to operating conditions. In the experimental work, according to Morales-Gómez [22], the quantities measured directly were pressure and bulk temperature. Therefore, several pressure meters and thermocouples can be used in the instrument, which operates under vacuum. Bourdon type, stainless steel 316 SS pressure meter was used, and its uncertainty was estimated to be less than ±0.5% for the full scale. The scale of the pressure meter was 762 mm Hg to 30 psi. Measurements of thermocouples, J type (iron-constantan), had an uncertainty of ±1.1℃. The quantity measured indirectly through refraction index (refractometer Abbe type) was the concentration of LiBr in LiBr + H_2O solution. The scale of the refractometer was 1.300–1.700 and the measurement uncertainty was estimated to be less than ±0.0002.

Table 1 shows the operational range for each variable of the system. The location of the measurement points of each instrument is shown in Fig. 4.

Table 3
Weights (*Wi*) to the four ANNs models which COP predicts 2 hidden neurons ($S = 2$ and input = 16)

Input	W (input, s) LOGSIG; 0 to 1		W (input, s) TANSIG; 0 to 1		W (input, s) TANSIG; −0.9 to 0.9		W (input, s) TANSIG; −0.6 to 0.6	
1	33.6	16.4	8.5504	−6.2313	0.6848	−0.3251	−0.2988	0.1307
2	−1.0	−3.1	−6.3929	2.2153	−0.0533	0.4442	−0.7064	−0.0865
3	−51.6	−43.6	−20.5207	14.3628	−0.4064	−0.3815	0.2873	−0.3623
4	5.5	6.0	2.6325	0.0127	0.0704	0.0672	−0.0537	0.0591
5	13.1	22.7	10.2056	−4.4762	0.2479	0.7343	0.0037	0.2266
6	−10.3	−4.4	1.1850	4.0309	0.0571	0.0075	0.0223	−0.0101
7	4.9	−0.2	0.8758	1.3760	−0.2094	0.0721	0.0350	−0.1249
8	−1.5	0.6	−3.1188	−5.2947	0.0114	−0.0864	−0.0646	0.2576
9	0.2	−0.1	0.0122	0.0956	0.1252	0.0026	0.0102	−0.0409
10	0.1	3.0	5.8843	−2.3629	−2.1100	−0.4140	0.7237	−0.0105
11	−1,281.8	199.7	−4.2614	−169.2125	2.4558	−0.9084	0.4878	−3.7478
12	612.9	−10.7	36.8644	−195.4480	2.8075	0.6606	0.1787	0.1735
13	558.3	−29.1	5.2894	−200.1477	−3.3246	1.7219	−0.1819	−0.1122
14	−222.1	−171.1	−55.8610	120.3188	2.2428	−1.4973	−0.0579	1.8228
15	−37.5	5.8	−0.2825	−128.0459	0.0558	0.0535	−0.1877	0.8003
16	285.8	−30.8	7.1055	296.6966	0.2497	0.0803	0.0107	−0.0919

Table 4
Weights (*Wo*, and biases *b*1 and *b*2) to the four ANNs models which COP predicts 2 hidden neurons ($S = 2$ and input = 16)

LOGSIG; 0 to 1		TANSIG; 0 to 1		TANSIG; −0.9 to 0.9		TANSIG; −0.6 to 0.6	
W_o		W_o		W_o		W_o	
0.1096	0.2961	0.1453	−0.0589	−0.4528	0.9319	−1.3653	−0.4169
*b*1		*b*1		*b*1		*b*1	
84.3498		10.9363		0.3950		−0.1157	
37.1894		198.6711		−0.0087		0.1091	
*b*2		*b*2		*b*2		*b*2	
0.0421		0.2606		0.4615		0.1711	

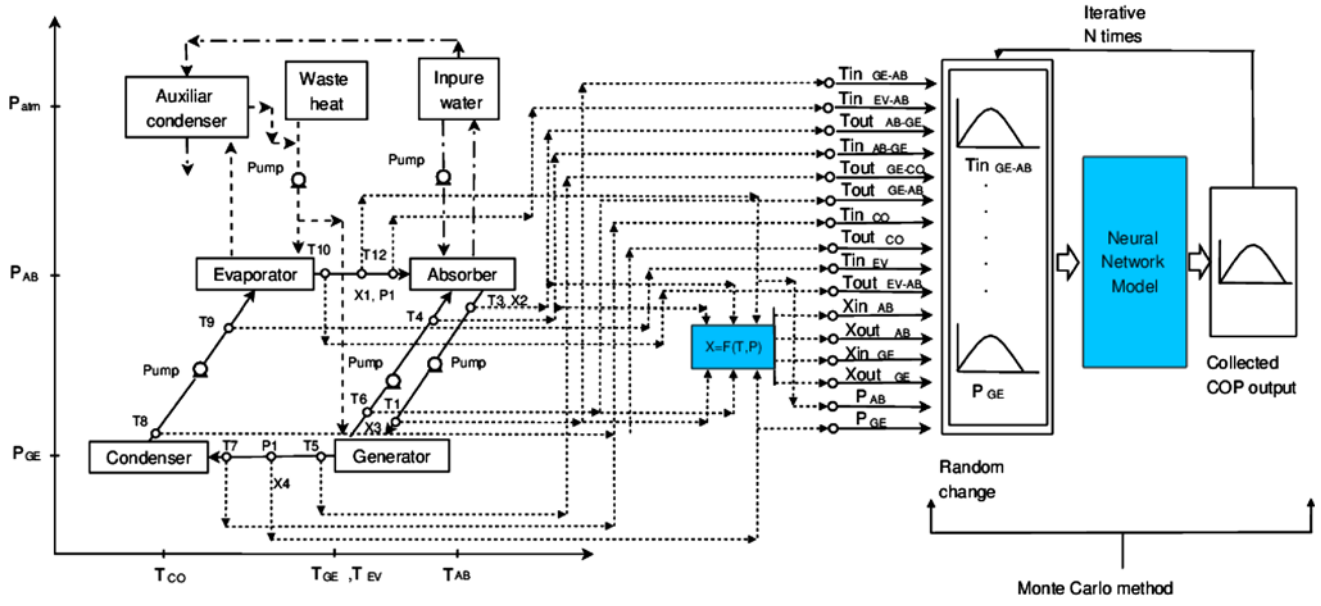

Fig. 4. Schematic representation of analyzed uncertainties on ANN model by the Monte Carlo method.

As the uncertainty limits of instrumentation can influence the accuracy of the COP calculation by the Monte Carlo method, generating random numbers from a normal distribution to evaluate the input variables in artificial neural network model. In this work, the range reported for a parameter can be considered equal to six standard deviations.

We used the relative standard deviation (%RSD) for the error incorporated in the operation variables (temperature, pressure and concentration). Relative standard deviation is determined as follows:

$$\%\mathrm{RSD}_{\mathrm{instrument}} = \frac{100\sigma_{\mathrm{input}}}{\bar{x}_{\mathrm{input}}} \tag{11}$$

The error propagation in COP prediction by the neural network model is defined by uncertainty limits of instrumentation, its characteristics for prediction and operation levels. A neural network consists of a nonlinear model where the correlation structure is very important. In this work, different levels of uncertainty in the input layer of neural network were used to determine effects over COP prediction uncertainty.

The error propagation in COP prediction by the ANN model is defined by uncertainty limits of instrumentation, its prediction characteristics and operational levels. The iterative model used to determine error propagation has the following sequence:

- Specify the uncertainty limit of the input layer (temperature, pressure and concentration) of neural network. Because the actual error estimates were not available, we assumed two extreme cases for instrumental measurement errors: (i) %RSD = 1 and (ii) %RSD = 0.1. We considered the errors in case (i) as "typical" errors, which might be representative of a routine experiment of the heat transformer, and those in case (ii) as typically obtainable errors in well-designed experiments using high-precision equipment [25].
- Generate random numbers with normal distribution from the average and standard deviation of every operational variable.
- Simulate COP prediction with ANN model.
- Determine the standard deviation and average of COP-predicted distribution.

5. Approximation analyses

This section describes the results obtained for each neural network model and the obtained statistical information in the validation process.

Analysis between ANN-simulated and experimental data is evaluated through the residual sum of squares (RSS). The RSS is given by

$$\mathrm{RSS} = \sum_{i=1}^{n} (\mathrm{COP}_{\mathrm{sim}} - \mathrm{COP}_{\mathrm{exp}})^2 \tag{12}$$

Nonparametric statistical analysis based on the absolute value of difference between experimental and ANN-simulated frequencies was used. In this work, the sum of residuals (X_i) is given by

$$X_i = \sum_{i=1}^{n} \frac{(\mathrm{COP}_{\mathrm{sim}} - \mathrm{COP}_{\mathrm{exp}})^2}{\mathrm{COP}_{\mathrm{exp}}} \tag{13}$$

Table 5 shows the results with statistical tools. RSS values to 0.0816 and the sum of residuals $X_i = 0.2577$ showed lower values for the ANN with TANSIG transfer function in the hidden layer model in comparison with other cases that were evaluated. Therefore, this option better adjusted the experimental data to the proposed ANN model using a normalization range from −1 to 1. The statistical results of the intercept and the slope in the validation process confirm the conclusion.

Consequently, an ANN model for a water purification process integrated into heat transformer considering normalization range from −1 to 1, TANSIG function transfer and two neurons in the hidden layer is a good option to predict COP without uncertainty in the input variables. In this analysis, for models with TANSIG in the hidden layer, when the normalization range is increased, the R values are increased, RSS is decreased, and therefore, the X_i values and the quality of validation are better. Afterward, we evaluated the confidence level of the models using Monte Carlo method for the error propagation in the prediction.

6. Uncertainty analyses

Based on the above-mentioned mathematical model (ANN) and the methodology showed in the section Error propagation, a code has been developed to determine standard deviation of predicted COP. The code has been carefully verified using, whenever possible, Bevington and Robinson [18] equations. Excellent agreement is found between the average and standard deviation.

The Monte Carlo method with 100,000 random numbers and $\%\mathrm{RSD}_{\mathrm{instrument}}$ of 0.5 and a neural network model are compared with experimental data obtained by [22] in Table 6. Numerical prediction had a discrepancy lower than 0.1% for LOGSIG with a normalization range from 0 to 1, lower than 13% for TANSIG with a normalization range from 0 to 1, lower than 32% for TANSIG with a normalization range from −0.9 to 0.9 and lower than 7.7% for TANSIG with a normalization range from −0.6 to 0.6 with regard to experimental results. Neural network model

Table 5
Statistical analysis between simulated and experimental data

ANN models	RSS	X_i	R	Intercept	Slope
LOGSIG; 0 to 1	0.0835	0.2663	0.9978	0.0009 ± 0.0006	0.9972 ± 0.0021
TANSIG; 0 to 1	0.2166	0.6799	0.9943	0.0038 ± 0.0011	0.9885 ± 0.0033
TANSIG; −0.9 to 0.9	0.0816	0.2577	0.9979	0.0007 ± 0.0006	0.9975 ± 0.0020
TANSIG; −0.6 to 0.6	0.1280	0.4077	0.9967	0.0019 ± 0.0008	0.9943 ± 0.0026

Table 6
Comparision of simulated and experimental values of COP

		A	B	C	D	E	F	G
	COP_{EXP}	0.2100	0.2400	0.2700	0.3000	0.3300	0.3600	0.3900
LOGSIG	COP_{SIM}	0.216	0.241	0.2664	0.2893	0.3183	0.3363	0.3523
0–1	$Error_{COP}$	0.0285	0.0041	0.0133	0.0356	0.0354	0.0658	0.0966
	σ_{COP}	0.0543	0.0601	0.0644	0.0661	0.0654	0.0631	0.0491
	$\%RSD_{COP}$	25.1388	24.9377	24.1741	22.8482	20.5466	18.7630	13.9369
TANSIG	COP_{SIM}	0.2371	0.2635	0.2868	0.307	0.3329	0.348	0.381
0–1	$Error_{COP}$	12.9047	9.7916	6.2222	2.3333	0.8787	3.3333	2.3076
	σ_{COP}	0.0309	0.038	0.0417	0.0433	0.0434	0.0422	0.0368
	$\%RSD_{COP}$	13.0324	14.4212	14.5397	14.1042	13.0369	12.1264	9.6587
TANSIG	COP_{SIM}	0.2129	0.2466	0.2730	0.2966	0.3289	0.3493	0.3790
−0.9–0.9	$Error_{COP}$	31.0476	27.8750	23.5925	19.1667	17.8787	13.5277	11.0769
	σ_{COP}	0.1266	0.1332	0.1336	0.1339	0.1337	0.1329	0.1238
	$\%RSD_{COP}$	46.0029	43.4017	40.0359	37.4545	34.3701	32.5177	28.5780
TANSIG	COP_{SIM}	0.2000	0.2216	0.2527	0.2797	0.3138	0.3375	0.3635
−0.6–0.6	$Error_{COP}$	4.7619	7.6666	6.4074	6.7666	4.9090	6.2500	6.7948
	σ_{COP}	0.0684	0.0688	0.0706	0.0722	0.0746	0.0761	0.0942
	$\%RSD_{COP}$	34.2000	31.0469	27.9382	25.8133	23.7731	22.5481	25.9147

with Monte Carlo method exhibited a satisfactory ability for COP prediction for ANN models developed. However, the model with TANSIG in the hidden layer and normalization range from −1 to 1 presents a high discrepancy between the predictions and experimental COP (up to 31%). Especially, it is very interesting to incorporate a standard deviation for each test (see Table 6). Standard deviation for LOGSIG with a normalization range from 0 to 1 is lower than 0.07, for TANSIG with a normalization range from 0 to 1 is lower than 0.045, for TANSIG with a normalization range from -0.9 to 0.9 is lower than 0.134 and for TANSIG with a normalization range from −0.6 to 0.6 is lower than 0.095.

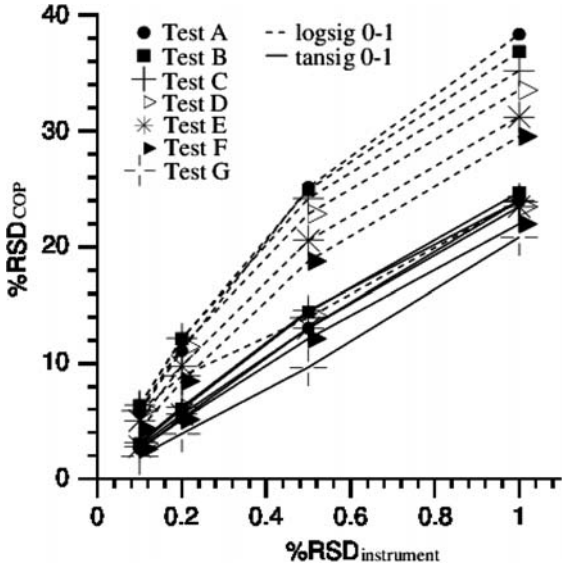

Fig. 5. %Rsdcop against $\%RSD_{instrument}$ for all data base with 100,000 random numbers using different functions in the hidden layer.

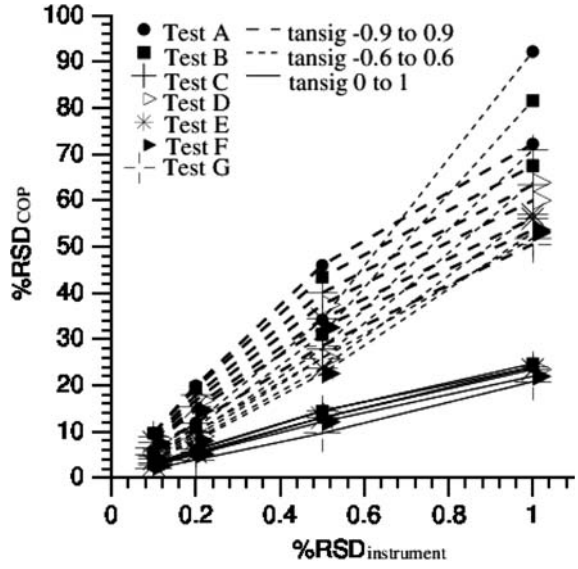

Fig. 6. %Rsdcop against $\%RSD_{instrument}$ for all data base with 100,000 random numbers using different normalization range.

Fig. 5 shows a $\%RSD_{COP}$ for each COP_{EXP} with variations in $\%RSD_{instrument}$ using LOGSIG and TANSIG in the hidden layer of ANN. According to the comparison in Fig. 5, the $\%RSD_{COP}$ decreases when the COP increased. The first ANN model developed with LOGSIG in the hidden layer presents %RSD up to 38.3 for low COP values, whereas the second ANN model developed with TANSIG in the hidden layer with input normalization range between 0 and 1 presents %RSD up to 23.9 for low COP values. Nevertheless, the first ANN model with LOGSIG in the hidden layer for high COP presents %RSD similar to the second ANN model with TANSIG in the hidden layer for low COP.

With the aim to evaluate the influence of the normalization process in TANSIG transfer function over error estimation COP, three different normalization ranges were evaluated. According to Eqs. (6), (9) and (10), input variables to ANN models were normalized. Fig. 6 shows a $\%RSD_{COP}$ for each COP_{EXP} with variations in $\%RSD_{instrument}$ using TANSIG in the hidden layer of ANN and different normalization ranges. The third ANN model developed with TANSIG in the hidden layer with input normalization range from −0.9 to 0.9 presented a %RSD up to 72.2 for low COP values. The fourth ANN model with input normalization range from −0.6 to 0.6 presented a %RSD up to 92.2 for low COP. The reduction in the normalization

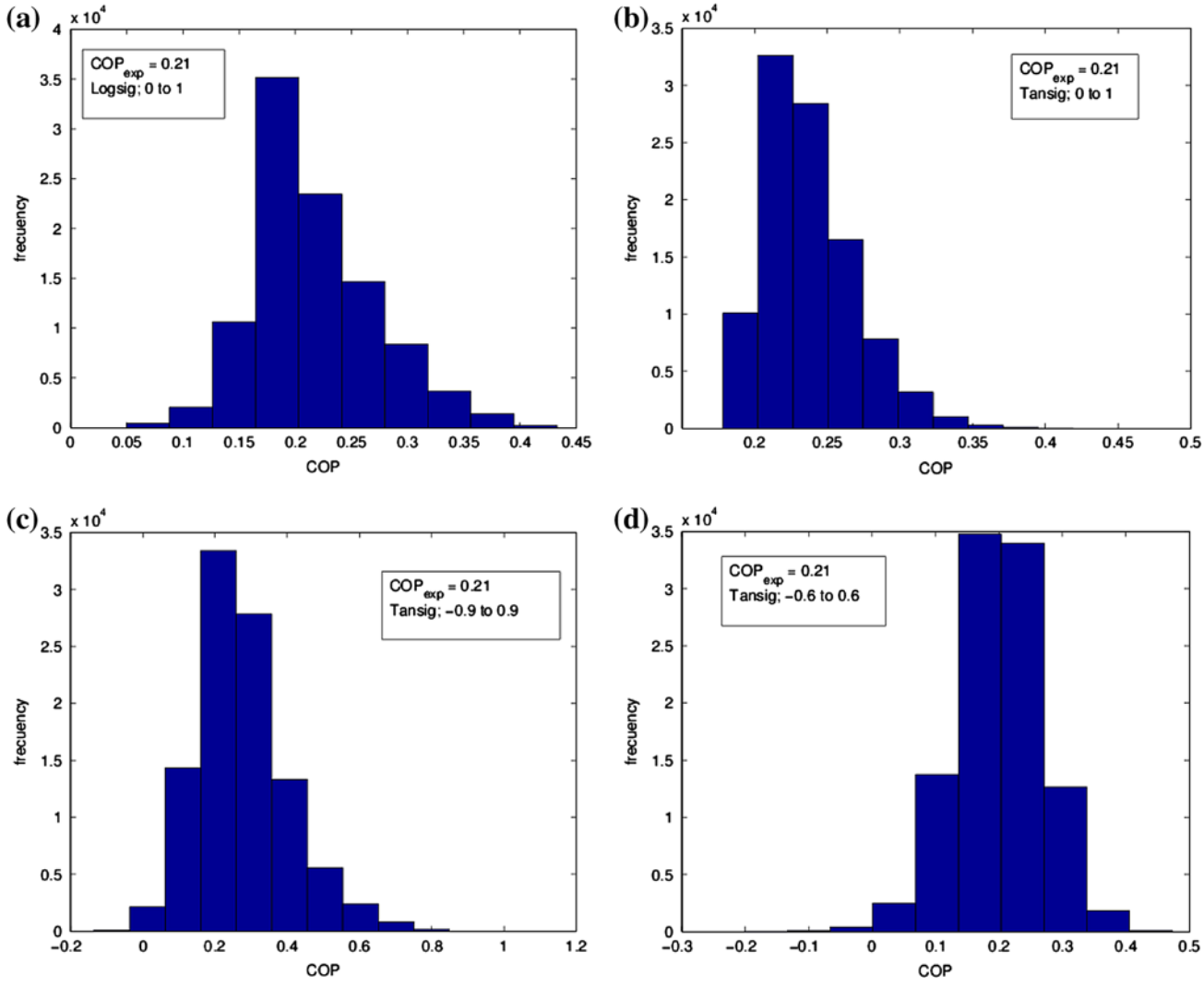

Fig. 7. Histogram of distribution using conditions for $COP_{exp} = 0.21$. (a) using LOGSIG in the hidden layer, and normalization range from 0 to 1. (b) Using TANSIG in the hidden layer, and normalization range from 0 to 1. (c) Using TANSIG in the hidden layer, and normalization range from -0.9 to 0.9. (d) Using TANSIG in the hidden layer, and normalization range from −0.6 to 0.6.

range decreased the %RSD in the COP prediction. The second ANN model developed with TANSIG in the hidden layer and input normalization from 0 to 1 presented a %RSD up to 24 for low COP values.

Fig. 7 shows the distributions of COP simulated with each ANN developed for $COP_{exp} = 0.21$ (see test A of Table 2). These conditions are selected as they make more effective the discrepancy in COP simulated with respect to a COP experimental (see Table 6). Colorado et al. [21] described the output COP simulates as a normal distribution. Nevertheless, in this case, one statistical analysis based on tests to distribution is necessary for each output COP, aimed to determine whether output COP presented in each neural model is normal or the other type (for instance, positive skew). In this way, open issues to improve this comparison are given by a correct definition of %RSD in function of other measures of central tendency (for instance, mode). On the other hand, the equations presented in this work to evaluate normalization process could be compared with those proposed by Khataee and Mirzajani [26] in order to find an optimum normalization range for the performance prediction of heat pumps.

7. Conclusion

Four feedforward neural networks were obtained and compared satisfactorily. For the comparison without considering uncertainty in the input variables the ANN model with normalization range between −1 and 1 and TANSIG function transfer in the hidden layer represents a good option to predict COP.

Error propagation from Monte Carlo technique applied on COP prediction by ANNs in a water purification system integrated into an absorption heat transformer has been successfully developed using different transfer functions in the hidden layer and normalization range. The Monte Carlo method appears to offer a reasonable approach to the analysis of error propagation COP with an efficient computing complexity.

However, an ANN with TANSIG in the hidden layer with input normalization range from 0 to 1 presents lower %RSD than other alternatives evaluated in a water purification system integrated into an absorption heat transformer. An ANN with LOGSIG in the hidden layer with input normalization range from 0 to 1 presents the lowest %RSD for high values of COP and low values for RSS and X_i; therefore, it is an advisable option. Error level is high for an experimental measurement for ANN models. Therefore, it is important to work with a level less than 0.5 of uncertainty in the instruments or a higher level of COP_{exp}. Normalization range of input variables influences the $\%RSD_{COP}$ prediction. In this work, input normalization range from 0 to 1 presented better results in comparison with other normalization ranges. Studies about input and output distributions and those evaluating error propagation of neural networks models are necessary for other energy systems.

Symbols

$b1$, $b2$	—	matrix of bias
COP	—	coefficient of performance
f	—	transfer function for neural network
g	—	transfer function (linear) for neural network
H	—	specific enthalpy, kJ/kg
IR	—	refraction index
In	—	input variable
K	—	input number
LOGSIG	—	logarithmic sigmoid transfer function
ns, n	—	neurons in the hidden layer
Out	—	output variable
P	—	pressure, inHg
Q	—	heat flow, W
R	—	regression coefficient
RSD	—	relative standard deviation
T	—	temperature, ℃
TANSIG	—	hyperbolic tangential transfer function in the hidden layer
TinCO (cooling)	—	input temperature of cooling fluid in the condenser, ℃
ToutCO (cooling)	—	output temperature of cooling fluid in the condenser, ℃
TinEV (heating)	—	input temperature of heating fluid in the evaporator, ℃
ToutEV (heating)	—	output temperature of heating fluid in the evaporator, ℃
X	—	concentration, %w/w
x	—	average
WP	—	water purification
Wi, Wo	—	matrix weight
Greek letters		
ϕ	—	operation variable
σ	—	standard deviation
Inlet variables for ANN		
TinGE-AB	—	input temperature in the absorber that comes from the generator, ℃
TinEV-AB	—	input temperature in the absorber that comes from the evaporator, ℃
ToutAB-GE	—	output temperature from the absorber into the generator, ℃
TinAB-GE	—	Input temperature in the generator that comes from the absorber, ℃

ToutGE-CO — output temperature in the generator toward the condenser, ℃
ToutGE-AB — output temperature in the generator toward the absorber, ℃
TinCO — input temperature of the condenser that comes from the generator, ℃
ToutCO — output temperature in the condenser toward the evaporator, ℃
TinEV — input temperature in the evaporator that comes from the condenser, ℃
ToutEV — output temperature in the evaporator toward the absorber, ℃
PAB and PGE — pressures in the absorber and the generator, respectively, inHg
XinAB — LiBr input concentration to the absorber, %w/w
XinGE — LiBr input concentration to the generator, %w/w
XoutAB — LiBr output concentration to the absorber, %w/w
XoutGE — LiBr output concentration to the generator, %w/w

Subscript

AB — absorber
CO — condenser
EV — evaporator
EXP — experiment
GE — generator
i — instrument
s — sensible
sim — simulated
MC — Monte Carlo method
v — latent

References

[1] S.A. Kalogirou, Applications of artificial neural-networks for energy systems, Appl. Energy 67 (2000) 17–35.
[2] S.A. Kalogirou, Applications of artificial neural networks in energy systems: a review, Energy Convers. Manage. 40 (1999) 1073–1087.
[3] J.A. Hernández, M.A. García-Alvarado, G. Trystram, B. Heyd, Neural networks for the heat and mass transfer prediction during drying of cassava and mango, Innovat. Food Sci. Emerg. Technol. 5 (2004) 57–64.
[4] L. Díaz-González, E. Santoyo, J. Reyes-Reyes, Three new Na/K geothermometer using computational tools and geochemometrics: application of geothermal system temperature prediction, Revista Mexicana de Ciencias Geológicas 25 (2008) 465–482.
[5] J.A. Hernández, D. Juarez-Romero, L.I. Morales, J. Siqueiros, COP prediction for the integration of a water purification process in a heat transformer: with and without energy recycling, Desalination 219 (2008) 66–80.
[6] Gao Penghui, Zhang Lixi, Cheng Ke, Zhang Hefei, A new approach to performance analysis of a seawater desalination system by an artificial neural network, Desalination 205 (2007) 147–155.
[7] N. Delgrange-Vincent, C. Cabassud, M. Cabassud, Durand-Bourlier, J.M. Laine, Neural networks for long term prediction of fouling and backwash efficiency in ultrafiltration for drinking water production, Desalination 131 (2000) 353–362.
[8] F.A. Holland, J. Siqueiros, S. Santoyo, C.L. Heard, E. Santoyo, Water purification using heat pumps, E&FN Spon, London, 1999.
[9] S. Santoyo-Gutiérrez, J. Siqueiros, C. Heard, E. Santoyo, F.A. Holland, An experimental integrated absorption heat pump effluent purification system. Part I: operating on water/lithium bromide solutions, Appl. Therm. Eng. 19 (1999) 461–475.
[10] W. Rivera, Experimental evaluation of a single-stage heat transformer used to increase solar pond's temperature, Sol. Energy 69(5) (2000) 369–376.
[11] J. Siqueiros, R.J. Romero, Increase of COP for heat transformer in water purification systems. Part I – increasing heat source temperature, Appl. Therm. Eng. 27 (2007) 1042–1053.
[12] A. Huicochea, J. Siqueiros, Improved efficiency of energy use of a heat transformer using a water purification system, Desalination 14 (1994) 336–427.
[13] J.A. Hernández, A. Bassam, J. Siqueiros, D. Juárez-Romero, Optimum operating conditions for a water purification process integrated to a heat transformer with energy recycling using neural networks inverse, Renew. Energy 34 (2009) 1084–1091.
[14] A. Sozen, E. Arcaklioglu, Exergy analysis of an ejector-absorption heat transformer using artificial neural network approach, Appl. Therm. Eng. 27 (2007) 481–491.
[15] M. Mohanraj, S. Jayaraj, C. Muraleedharan, Performance prediction of a direct expansion solar assisted heat pump using artificial neural networks, Energy 86 (2009) 1442–1449.
[16] H. Esen, M. Inalli, A. Sengur, M. Esen, Forecasting of a ground-coupled heat pump perfomance using neural networks with statistical data weighting pre-processing, Int. J. Therm. Sci. 47 (2008) 431–441.
[17] H. Esen, M. Inalli, ANN and ANFIS models for performance evaluation of a vertical ground source heat pump system, Expert Syst. Appl. 37 (2010) 8134–8147.
[18] P.R. Bevington, D.K. Robinson, Data reduction and error analysis for the physical science, third ed., McGrawHill, New York, NY, 2003.
[19] G.M. Anderson, Error propagation by the Monte Carlo method in geochemical calculations, Geochim. Cosmochim. Acta 40 (1976) 1533–1538.
[20] C.E. Rees, Error propagation calculations, Geochim. Cosmochim. Acta 48 (1984) 2309–2311.
[21] D. Colorado, J.A. Hernández, Y. El Hamzaoui, A. Bassam, J. Siqueiros, J. Andaverde, Error propagation on COP prediction by artificial neural networks in a water purification system integrated to an absorption heat transformer, Renew. Energy 36 (2011) 1315–1322.
[22] L.I. Morales-Gómez, Experimental study of a portable water purification system integrated to heat transformer, MSc Thesis, México, CIICAp-UAEM, 2005.
[23] J. Torres-Merino, Liquid-gas heat exchanger without contact for multi-stage absorption heat pumps, PhD Thesis, National Polytechnic Institute of Lorraine, France, 1997.
[24] S.P. Verma, Optimization of the exploration and evacuation of geothermal resource, In: D. Chandrasekharam, J. Bundschuh (Eds.), Geothermal energy resources for developing countries, Swets and Zeitlinger, B.V., A.A. Balkerma, Rotterdam, 2002, pp. 195–224.
[25] S.P. Verma, J. Andaverde, E. Santoyo, Application of the error propagation theory in estimates of static formation temperatures in geothermal and petroleum boreholes, Energy Convers. Manage. 47 (2006) 3659–3671.
[26] A.R. Khataee, O. Mirzajani, UV/peroxydisulfate oxidation of C.I. Basic blue 3: modeling of key factors by artificial neural networks, Desalination 251 (2010) 64–69.